Preprints of the 21st IFAC World Congress (Virtual)
Berlin, Germany, July 12-17, 2020

Optimal Freewheeling Control of a Heavy-Duty Vehicle Using Mixed Integer Quadratic Programming

Manne Held [∗,∗∗] **Oscar Flärdh** [∗] **Fredrik Roos** [∗]
Jonas Mårtensson [∗∗]

[∗] *Scania CV AB, 151 87 Södertälje, Sweden*
[∗∗] *Division of Decision and Control Systems and the Integrated Transport Research Lab, KTH Royal Institute of Technology, 100 44 Stockholm, Sweden.*
e-mail: manneh@kth.se, oscar.flardh@scania.com, fredrik.roos@scania.com, jonas1@kth.se

Abstract: Improving the powertrain control of heavy-duty vehicles can be an efficient way to reduce the fuel consumption and thereby reduce both the operating cost and the environmental impact. One way of doing so is by using information about the upcoming driving conditions, known as look-ahead information, in order to coast in gear or to use freewheeling. Controllers using such techniques today mainly exist for vehicles in highway driving. This paper therefore targets how such control can be applied to vehicles with more variations in their velocity. The driving mission of such a vehicle is here formulated as an optimal control problem. The control variables are the tractive force, the braking force, and a Boolean variable representing closed or open powertrain. The problem is solved by a model predictive controller, which at each iteration solves a mixed integer quadratic program. The fuel consumption is compared for four different control policies: a benchmark following the reference of the driving cycle, look-ahead control without freewheeling, freewheeling with the engine idling, and freewheeling with the engine turned off. Simulations on a driving cycle with a varying velocity profile show the potential of saving 11 %, 19 %, and 23 % respectively for the control policies compared with the benchmark, in all cases without increasing the trip time.

Keywords: Predictive control, autonomous vehicles, optimal control, integer programming.

1. INTRODUCTION

The road freight sector accounts for nearly 6 % of the total CO_2 emissions in the EU (TNO, 2015). Therefore, the EU has agreed that emissions for new heavy-duty vehicles (HDVs) should be decreased compared to the 2019 level by 15 % in 2025 and by 30 % in 2030 (European Parliament, 2018). One way to decrease the emissions is to improve components, for instance by designing more efficient engines. Another way, which is the focus of this paper, is to improve the control of the vehicles by more fuel-efficient software.

Many HDVs are today equipped with speed controllers using look-ahead information, such as road grade, to drive in a more fuel-efficient way. One example is Scania active prediction (Scania CV AB, 2012), released in 2011, which can save 3 % fuel by adapting the speed profile to changes in the altitude. This is mainly done by coasting ahead of downhills in order to avoid braking. A few years later, freewheeling, i.e., decoupling the engine from the rest of the powertrain, was added to the controller. With this functionality, the fuel consumption was further reduced by 2 % (Scania CV AB, 2013). Even though controllers such as these already exist for commercial use, their applications are limited to driving conditions where the velocity only deviates by a few percent from a fixed set-point. This is typically the case for vehicles in highway driving. Many other vehicles, for instance in mining applications or vehicles delivering goods, typically have large variations in their velocity. For these vehicles, such controllers do not exist to the same extent, which is one motivation for the work in this paper.

The focus of this paper is fuel-efficient powertrain control of heavy-duty vehicles with varying velocity demands. An example of such a scenario can be seen in Fig. 1. The vehicle has access to information about the speed limits and the road grade of the upcoming downhill by using a map and GPS communication. While approaching new speed restrictions and sections with significant road grade, the vehicle can be controlled in different ways such as braking, coasting in gear and freewheeling. For fuel efficient driving, braking should in most cases be avoided, but deciding when to use coasting in gear and when to use freewheeling is not trivial. In addition, the decision may depend on whether the engine is idling or turned off during freewheeling.

Funding provided by Swedish Governmental Agency for Innovation Systems (VINNOVA) through the FFI program is gratefully acknowledged.

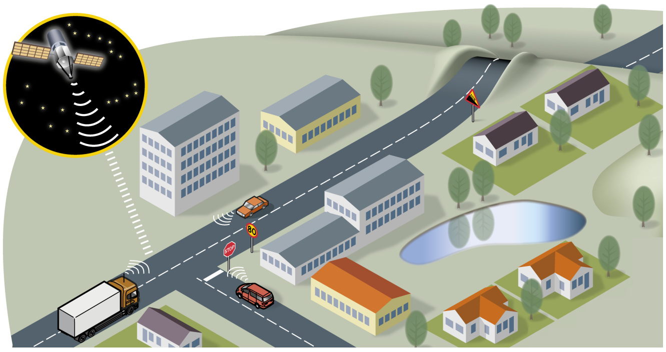

Fig. 1. A heavy-duty vehicle in a driving mission involving varying velocity constraints and significant road slope.

The approach for fuel reduction in this paper is, given a driving mission of a heavy-duty vehicle, to formulate it as an optimal control problem. This has previously been done in Held et al. (2019), where the problem was solved using both Pontryagin's Maximum Principle and Quadratic Programming (QP). The analysis was done from an energy perspective, and did not take the powertrain into account. Therefore, in this paper, a variable for whether the powertrain is closed or not is added to the QP-formulation. The main benefit of this is that the vehicle can save fuel by freewheeling with low engine speed and thus reduce the drag losses in the engine. With the new variable, the problem becomes a Mixed Integer Quadratic Program (MIQP).

Mixed integer programming has been used to solve similar problems before. A Model Predictive Controller (MPC) solving a mixed integer nonlinear program was applied to a heavy-duty vehicle in Kirches et al. (2011) in order to find the optimal gear shifting policy. The application was highway driving and freewheeling was not considered. Mixed integer programming has also been applied to the lateral movement of vehicles in order to avoid obstacles (Qian et al., 2016). Another application was made for trains in Wang et al. (2011), where a mixed integer formulation was used in order to approximate nonlinear functions by a piecewise affine function.

One method for reducing the fuel consumption of HDVs is to reduce the total energy lost due to drag losses in the engine by decreasing the engine speed. This can be done by alternating between tractive power and freewheeling, known as Pulse-and-Glide (PnG). Four different cases of PnG were specifically studied in Xu et al. (2015). One optimal cycle of PnG was performed for each case and they were then compared in terms of fuel consumption. External effects from road grade and varying velocity constraints, which might influence the timing of the PnG phases, were not considered. Another example is Li and Peng (2011), where PnG strategies were compared for different velocities in a car-following scenario. The engine drag torque at idling was not considered, and a continuous function could therefore be fitted to the fuel rate.

One motivation for the work in this paper is the potential of decreasing the fuel consumption by reducing the drag losses in the engine, i.e., the losses caused by friction and gas exchange etc. For these kind of losses, the potential savings increase with decreasing gear numbers. This is because lower gear numbers mean more revolutions of the engine for the same driven distance. The vehicles considered in this paper drive at lower velocities and thus lower gear numbers than vehicles in highway applications. Therefore, reducing the drag losses is even more important for such vehicles compared to vehicles in highway driving, for which controllers using PnG already exist commercially.

A similar problem to the one in this paper was solved in Henriksson et al. (2017) using Dynamic Programming (DP). The main drawback of using DP is that the computation time can be very large due to the curse of dimensionality, i.e., the fact that the computation time grows exponentially with the number of states and control signals. Furthermore, the velocity in Henriksson et al. (2017) is discretized and is thus no longer a continuous variable.

The main contributions of this paper are:

(1) To find the optimal control of an HDV with the possibility to coast in gear, freewheel with idle engine and freewheel with engine off, applied to a driving cycle with both significant road slope and varying velocity requirements.
(2) Compared to Henriksson et al. (2017), to solve the problem with continuous velocity, to avoid the curse of dimensionality and to investigate the effects of freewheeling with the engine off.

The outline of this paper is the following. The model of the vehicle and its engine is introduced in Section 2. The optimal control problem is presented in Section 3, followed by simulation results in Section 4, and conclusions in Section 5.

2. MODELLING

The vehicle model is first described in terms of external forces, constraints, and time consumption in Section 2.1. In Section 2.2, the drag losses in the engine are being modeled and the conversion from energy to fuel is discussed in Section 2.3.

2.1 Vehicle model

The kinetic energy

$$K(s) = mv^2(s)/2 \tag{1}$$

is used as state variable as a function of position s, with m being the vehicle mass and v the velocity. The dynamics of the vehicle are given by

$$\frac{dK(s)}{ds} = F_{fw}(s) + F_b(s) + F_a(K(s)) + F_r(s) + F_g(s) \tag{2}$$

where $F_{fw}(s)$ is the force at the flywheel, $F_b(s)$ the force caused by the brakes, $F_a(K(s))$ by the air resistance, $F_r(s)$ by the rolling resistance, and $F_g(s)$ by gravity. The resulting force on the flywheel is given by

$$F_{fw}(s) = \begin{cases} F_p(s) - F_{d_c} & \text{powertrain closed} \\ 0 & \text{powertrain open} \end{cases} \tag{3}$$

where $F_p(s)$ is the force at the piston of the engine generated by the combustion and F_{d_c} is the drag force for closed powertrain which is discussed further in section 2.2.

Table 1. Parameters related to the vehicle and the environment. The parameters for the drag torque are not given due to confidentiality.

Parameter	Value
m - vehicle mass	26 000 kg
$P_{p_{\max}}$ - maximum piston power	265 kW
$F_{p_{\max}}$ - maximum piston force	49 kN
$F_{b_{\max}}$ - maximum braking force	70 kN
r_w - wheel radius	0.5 m
c_d - air drag coefficient	0.5
ρ - air density	1.292 kg· m^{-3}
A_f - vehicle cross-sectional area	10 m^2
c_r - rolling resistance coefficient	0.006
ω_c - engine speed powertrain closed	1100 RPM
ω_o - engine speed powertrain open	idle 500 RPM engine off 0 RPM
J_e - moment of inertia engine	4 kg·m^2
$T_{d,0}$ - constant drag torque	n/a
$T_{d,1}$ - linear drag torque	n/a

In (2), $F_a(K(s))$ represents the air resistance such that

$$F_a(K(s)) = -\frac{\rho A_f c_d K(s)}{m} \tag{4}$$

where ρ is the air density, A_f is the vehicle frontal area, and c_d is the air drag coefficient. The contribution from rolling resistance is given by

$$F_r(s) = -mgc_r \cos(\alpha(s)) \tag{5}$$

where c_r is the coefficient for the rolling resistance, g is the gravitational constant and α is the road slope. The gravitational force $F_g(s)$ is given by

$$F_g(s) = -mg \sin(\alpha(s)). \tag{6}$$

The brake force in (2) is constrained by

$$-F_{b_{\max}} \leq F_b(s) \leq 0. \tag{7}$$

By writing the inverse of the velocity as

$$\frac{1}{v} = \sqrt{\frac{m}{2}} K^{-1/2}, \tag{8}$$

the force at the piston is constrained by the maximum power at the piston $P_{p_{\max}}$ as

$$F_p(s) \leq P_{p_{\max}} \sqrt{\frac{m}{2}} K^{-1/2}. \tag{9}$$

By driving a distance ds with velocity v, the consumed time dt using (8) becomes

$$\mathrm{d}t = \mathrm{d}s \sqrt{\frac{m}{2}} K^{-1/2}. \tag{10}$$

The parameters used in the vehicle model can be seen in Table 1.

2.2 Engine drag losses

The energy losses due to engine drag are modelled as a force F_d in (3). It can be calculated using the relation

$$F_d = \frac{P}{v} \tag{11}$$

where the power P is calculated from the engine drag torque $T_d(\omega)$ and engine speed ω as

$$P = T_d(\omega)\omega. \tag{12}$$

The drag torque can be modelled to be linear in engine speed such that

$$T_d(\omega) = T_{d,0} + T_{d,1}\omega \tag{13}$$

where $T_{d,0}$ and $T_{d,1}$ are found using least squares fit to experimental values from a Scania engine. Combining (8) and (11)-(13) gives

$$F_d = \begin{cases} (T_{d,0} + T_{d,1}\omega_c)\,\omega_c \sqrt{\frac{m}{2}} K^{-1/2} & \text{powertrain closed} \\ (T_{d,0} + T_{d,1}\omega_o)\,\omega_o \sqrt{\frac{m}{2}} K^{-1/2} & \text{powertrain open} \\ 0 & \text{engine off} \end{cases} \tag{14}$$

where ω_c is the engine speed with closed powertrain and ω_o is the engine speed with open powertrain. These are both set to constant values. For ω_c, this is a simplification since it varies continuously between gear changes. The range of typically used engine speeds for HDVs is about 800-1500 RPM and thus much smaller than the range used by engines in personal cars. The chosen value of ω_c =1100 RPM is a commonly used and efficient engine speed. The Boolean variable $z \in \{0, 1\}$ is introduced such that it attains the value $z = 1$ if the powertrain is closed and $z = 0$ if the powertrain is open. The force at the piston is non-negative and can attain values up to its maximum $F_{p_{\max}}$ only if the powertrain is closed. If the constraint

$$0 \leq F_p(s) \leq F_{p_{\max}} z \tag{15}$$

is introduced, then (3) can be written

$$F_{fw}(s) = F_p(s) - F_{d_c} z. \tag{16}$$

The piston force F_p and its maximum value $F_{p_{\max}}$ are expressed in terms of the force they generate at the wheel. The work done by this force is given by multiplication by the distance at the wheel, which is the distance driven by the vehicle.

When the powertrain is open, the engine is either turned off or runs at idle. The energy needed for this is represented by the constant drag force F_{d_o}, which is taken into account in the cost function of the optimal control problem.

2.3 Energy to fuel

The vehicle has so far been modelled from an energy perspective. At the end of the day however, fuel consumption is what matters to the haulers. The fuel that is combusted in the engine performs a work that is transferred to the piston. As discussed in Heywood (1988), not all this work is available at the flywheel. The difference between the energy transformed to the piston and the one measured at the flywheel is a friction work. This work consists mainly of overcoming resistance due to relative movement of parts in the engine, but also of gas-exchange and auxiliaries. These losses are modelled through the drag forces F_{d_c} and F_{d_o} in this paper. Because of this, what is needed to calculate the fuel consumption is to convert to fuel, the work done by the forces at the piston: F_p when the powertrain is closed and F_{d_o} when the powertrain is open. The work done by these forces is made using different engine speed and torque. However, the efficiency with which fuel is transformed to energy at the piston, the *combustion efficiency*, differs only within the measurement uncertainty. Therefore, all energy transformed at the piston is here modelled to have the same efficiency. This means that even though the optimal control problem is modelled to minimize the energy consumption, it is equivalent to minimizing the fuel consumption.

Table 2. Settings for creating the velocity corridor.

	Benchmark	Policy 2-4
Δv [km/h]	1	4
n_Σ [-]	0.5	1
a_l [m/s^2]	0.3	0.25
a_u [m/s^2]	0.4	0.6

3. PROBLEM FORMULATION

This section first describes how the constraints on velocity are set based on the driving cycle and statistics from real HDV operations. Next, the problem is formulated and solved as an MIQP.

3.1 Velocity constraints

The driving cycle used for the simulations in this paper is based on a cycle with frequent velocity variations used at Scania CV AB. The cycle contains the road grade and a piecewise constant velocity reference. The original cycle contains a few stretches where the velocity is constant for more than 1 km. Such stretches are here reduced to be only 1 km long. The motivation for this removal is that look-ahead control with constant velocity profile is already a well-studied topic, see for instance Hellström et al. (2009).

The constraints on the velocity are set based on the method introduced in Held et al. (2019). In that paper, a statistical analysis was performed to find average and standard deviation of decelerations of HDVs for different start and end velocities. Now in this paper, these data are fitted to a 2-dimensional polynomial using a least squares method such that the average deceleration $d_\mu(v_1, v_2)$ in m/s^2 when decelerating from v_1 to v_2 in m/s is given by

$$\begin{aligned} d_\mu(v_1, v_2) = 0.366 + 0.0771v_1 - 0.0849v_2 \\ -0.00185v_1^2 + 0.00348v_1v_2 - 0.00214v_2^2 \end{aligned} \quad (17)$$

and the corresponding standard deviation $\Sigma(v_1, v_2)$ is given by

$$\begin{aligned} \Sigma(v_1, v_2) = 0.187 + 0.0250v_1 - 0.0327v_2 \\ -0.000734v_1^2 + 0.00187v_1v_2 - 0.00101v_2^2. \end{aligned} \quad (18)$$

These functions are used to create a velocity corridor, i.e., a lower and an upper constraint v_l and v_u for the velocity. Following the methods developed in Held et al. (2019), the procedure can be summarized as follows:

(1) Starting with a piecewise constant velocity reference v_{ref} given by the driving cycle.
(2) Set $v_l = v_{\text{ref}} - \Delta v$.
(3) Set $v_u = v_{\text{ref}} + \Delta v$.
(4) For each deceleration from v_1 to v_2, set v_l according to the deceleration $d_\mu(v_1, v_2) - n_\Sigma \Sigma(v_1, v_2)$ and v_u according to the deceleration $d_\mu(v_1, v_2) + n_\Sigma \Sigma(v_1, v_2)$, with d_μ and n_Σ given by (17) and (18).
(5) For each acceleration, set v_l and v_u such that they follow the constant acceleration a_l and a_u respectively.

In the algorithm above, Δv and n_Σ are settings for the width of the corridor in terms of deviation during constant velocity and during deceleration respectively.

Four different control policies are evaluated and compared in terms of their fuel consumption:

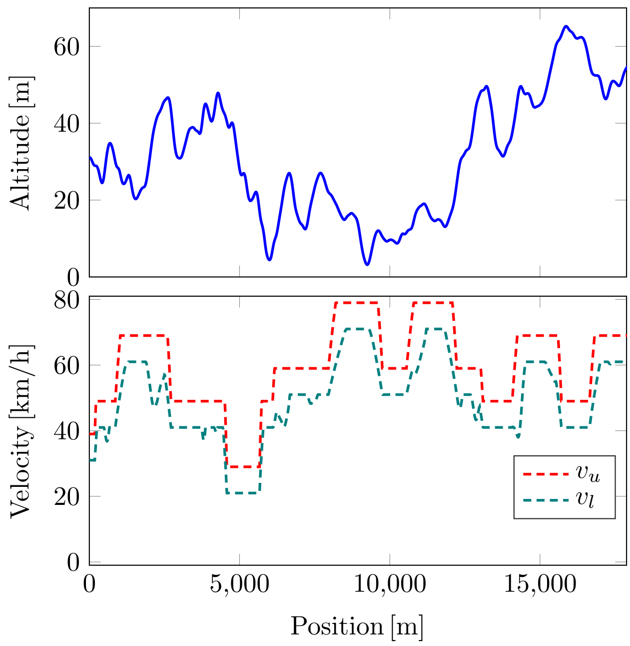

Fig. 2. The altitude of the driving cycle in the top figure and the velocity corridor in the bottom figure.

(1) Benchmark, no freewheeling,
(2) No freewheeling,
(3) Freewheeling with idling engine,
(4) Freewheeling with engine off.

For policy 2-4, the velocity corridor is constructed according to the steps above using the parameters in the right column of Table 2. The benchmark policy is derived by solving the same optimal control problem without the possibility to freewheel. In addition, the velocity corridor is very narrow, such that the velocity only deviates slightly from the reference of the driving cycle. The parameters for the benchmark solution are given in the left column of Table 2.

The road grade of the driving cycle has a maximum inclination of 4.3 % in an uphill. Such sections can possibly reduce the velocity of the vehicle significantly. Setting the lower velocity constraint directly as above might therefore result in infeasibility. To mitigate this, the lower constraint is modified in order to always contain a feasible solution. This is done by discretizing the constraint and for each step k setting

$$v_l[k] = \min\left(v_l[k], v_l[k-1] + \Delta v_l\right) \quad (19)$$

where Δv_l is the acceleration yielded by maximum tractive power. The altitude and the resulting velocity constraints can be seen in Fig. 2.

3.2 Mixed Integer Quadratic Program

The problem is discretized with $\Delta s = 15$ m using zero order hold and formulated as an MIQP. In order to do this, the cost function needs to be quadratic in the continuous state and control variables, the constraints need to be linear, and a continuous variable cannot be multiplied by the Boolean variable. The time consumption (10) is used in the cost function while (9) and (16) are used as constraints. They all contain the expression $K^{-1/2}$, and need to be approximated by the second, first, and zeroth order Taylor approximation respectively.

The second order Taylor approximation of the inverse of the square root of the kinetic energy around a reference trajectory K_r is given by

$$K^{-1/2} \approx K_r^{-1/2} - \frac{1}{2}K_r^{-3/2}(K - K_r) + \frac{3}{8}K_r^{-5/2}(K - K_r)^2. \tag{20}$$

The Taylor approximations of different degrees at step k become

$$K_k^{-1/2} \approx \begin{cases} \theta_{0,k} + \theta_{1,k}K_k + \theta_{2,k}K_k^2 & \text{second order} \\ \phi_{0,k} + \phi_{1,k}K_k & \text{first order} \\ \varphi_{0,k} & \text{zeroth order,} \end{cases} \tag{21}$$

where the second order coefficients are given by

$$\theta_{0,k} = \frac{15}{8}\sqrt{\frac{m}{2}}K_{r,k}^{-1/2} \tag{22a}$$

$$\theta_{1,k} = -\frac{10}{8}\sqrt{\frac{m}{2}}K_{r,k}^{-3/2} \tag{22b}$$

$$\theta_{2,k} = \frac{3}{8}\sqrt{\frac{m}{2}}K_{r,k}^{-5/2}, \tag{22c}$$

the first order coefficients are given by

$$\phi_{0,k} = \frac{3}{2}\sqrt{\frac{m}{2}}K_{r,k}^{-1/2} \tag{23a}$$

$$\phi_{1,k} = -\frac{1}{2}\sqrt{\frac{m}{2}}K_{r,k}^{-3/2}, \tag{23b}$$

and the zeroth order coefficient is given by

$$\varphi_{0,k} = \sqrt{\frac{m}{2}}K_{r,k}^{-1/2}. \tag{24}$$

The optimal control problem is solved in a receding horizon approach using an MPC with a control horizon of $N_H = 60$ steps. This leads to a control horizon with distance $\Delta s N_H = 900$ m which is enough for reaching the optimum value within a few parts per thousand (Held et al., 2019). Solving the optimal control problem using an MPC instead of offline as an optimization problem is motivated by the MIQP-solver not converging to a solution within a reasonable amount of time when solving over the full driving distance.

For each discretized step k, the problem is formulated as an MIQP as:

$$\min_{F_p, F_b, z} \sum_{j=k}^{k+N_H-1} \Delta s \left(F_{p,j} + \omega_o T_d(\omega_o)\varphi_{0,j}(1 - z_j)\right) \tag{25a}$$

$$+ \beta_g \Delta z_j \tag{25b}$$

$$+ \beta_t \Delta s \left(\theta_{0,j} + \theta_{1,j}K_j + \theta_{2,j}K_j^2\right) \tag{25c}$$

$$- K_{k+N_H} \tag{25d}$$

$$\text{s.t.} \quad K_{j+1} = AK_j + B(F_{p,j} - F_{d_c,j}z_j + F_{b,j}) + w_j \tag{25e}$$

$$F_{d_c,j} = \omega_c T_d(\omega_c)\left(\phi_{0,j} + \phi_{1,j}K_j\right) \tag{25f}$$

$$K_{l,j} \leq K_j \leq K_{u,j} \tag{25g}$$

$$F_{p,j} \leq P_{p_{\max}}\left(\phi_{0,j} + \phi_{1,j}K_j\right) \tag{25h}$$

$$0 \leq F_{p,j} \leq z_j F_{p_{\max}} \tag{25i}$$

$$-F_{b_{\max}} \leq F_{b,j} \leq 0 \tag{25j}$$

$$K_k \text{ given} \tag{25k}$$

where A, B and w_j are given by

$$A = e^{-A_c \Delta s}, \tag{26a}$$

$$B = \frac{1}{A_c}(1 - A) \tag{26b}$$

$$w_j = -Bmg\left(\sin\alpha_j + c_r\cos\alpha_j\right) \tag{26c}$$

where A_c is the state dependent coefficient in the continuous model (2) which is given by (4) as

$$A_c = -\frac{\rho A_f c_d}{m}. \tag{27}$$

The cost function is the sum of the energy used for traction and idling (25a), the cost for gear changes (25b) with $\Delta z_j = |z_{j+1} - z_j|$, and the cost for time consumption (25c). The kinetic energy at the end of the horizon (25d) is added such that it is not always optimal to coast at the end of the horizon. The constraints consist of the dynamics of the vehicle (25e) with the drag force given by (25f), the constraints on velocity (25g), maximum power at the piston (25h), maximum force at the piston (25i), and maximum braking force (25j). The constant β_g in (25b) is a penalty for activating or deactivating freewheeling. The motivation for this penalty is that when again closing the powertrain, the rotational speed of the engine must be increased such that an amount of energy corresponding to the difference in rotational energy is consumed. Since both engaging and disengaging a gear is penalized in (25b), the difference in rotation energy is divided by two such that

$$\beta_g = \frac{1}{2}J_e\frac{\omega_c^2 - \omega_o^2}{2} \tag{28}$$

where J_e is the engine moment of inertia. For the policy with the engine off, ω_o in (28) is set to zero. The penalty for time consumption β_t in (25c) is set such that the different control policies obtain similar trip times in order to make a fair comparison of their fuel consumption.

4. SIMULATION RESULTS

Simulations were performed in Matlab using the toolbox Yalmip (Löfberg, 2004) with the solver Gurobi (Gurobi Optimization, 2018). The energy/fuel consumption can be seen in Fig. 4 for the four compared policies normalized with the consumption of the benchmark. The consumption is split into the parts originating from rolling resistance, air resistance, braking, engine drag, idling and freewheeling on/off. As can be seen, the losses due to rolling resistance is the same for all control policies and the losses due to air resistance only have small deviations. The savings by using a wider velocity corridor found by comparing policy 1 and 2 come from reduction of the losses due to braking, as found in Held et al. (2019).

The savings when allowing freewheeling come from reduction of engine drag. As can be seen, the losses due to braking actually increase when freewheeling with engine off compared to freewheeling with idling. This is because when freewheeling with idling, it is beneficial to stop freewheeling if braking is necessary. With the engine off on the other hand, the vehicle may continue to freewheel when braking, in order to avoid the penalty for gear changes. In

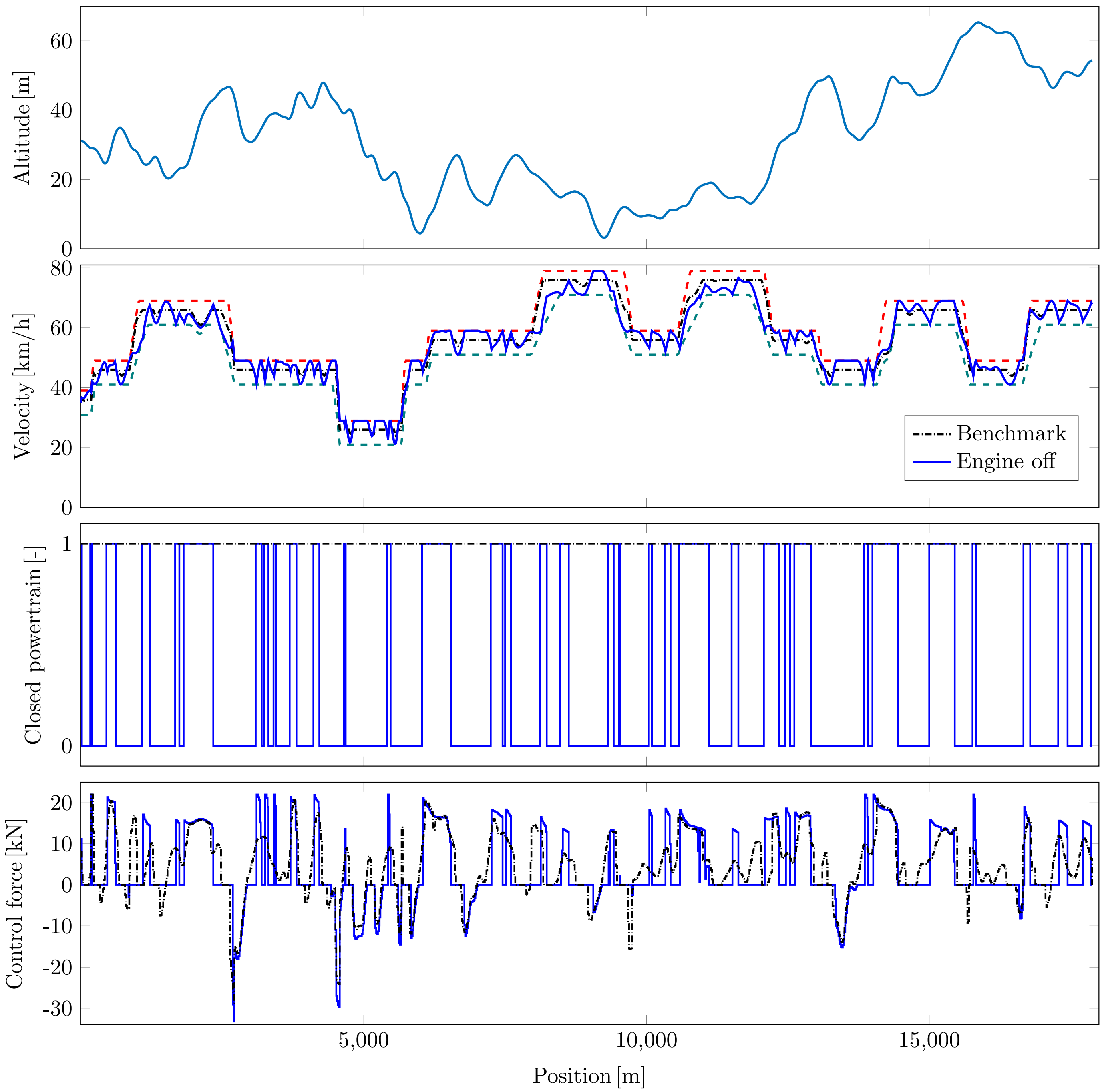

Fig. 3. Simulation results showing road altitude, velocity, closed powertrain, and control force.

the end, the sum of losses from braking and from engine drag are approximately the same for the two freewheeling policies. A summary of the resulting normalized fuel consumption together with the corresponding trip time can be seen in Table 3.

The resulting trajectories can be seen in Fig. 3 for the benchmark and for freewheeling with engine off. It can be seen that by using the latter control policy, the vehicle lowers the velocity ahead of downhills in order to avoid braking. The difference with the benchmark can be seen in the force plot at three locations during the first two kilometers. Fuel is also saved by using PnG which can be seen in the frequent switching in the powertrain plot, even at locations without significant changes in altitude.

Table 3. Resulting fuel consumption and trip time as percentage of the benchmark for the different control policies.

	Bench.	No freew.	Idling	Eng. off
Fuel [%]	100	88.8	81.5	77.1
Time [%]	100	99.4	99.7	99.7

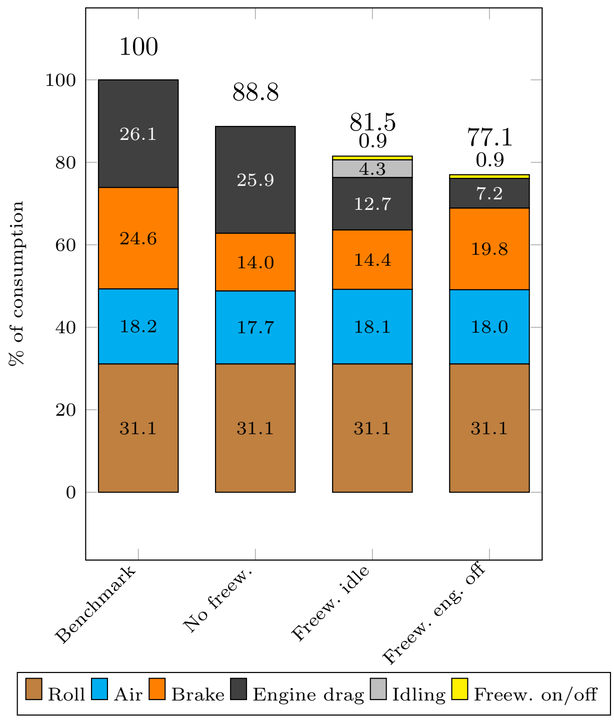

Fig. 4. Losses divided into categories for the different control policies.

5. CONCLUSIONS

The driving mission of a heavy-duty vehicle with varying velocity demands is formulated as an optimal control problem on MIQP form. The fuel savings for the four different control policies are: 11.2 % for look-ahead control without freewheeling, 18.5 % for freewheeling with the engine idling, and 22.9 % for freewheeling with the engine turned off. These results indicate great potential in fuel savings by using look-ahead control for applications with large velocity variations. However, the fuel savings in real driving might be less due to simplifications in the vehicle model and the presence of other traffic participants.

REFERENCES

European Parliament (2018). CO2 emission standards for heavy-duty vehicles. URL `https://www.europarl.europa.eu/RegData/etudes/BRIE/2018/628268/EPRS_BRI(2018)628268_EN.pdf`.

Gurobi Optimization (2018). Gurobi Optimizer Reference Manual. URL `http://www.gurobi.com`.

Held, M., Flärdh, O., and Mårtensson, J. (2019). Optimal Speed Control of a Heavy-Duty Vehicle in Urban Driving. *IEEE Transactions on Intelligent Transportation Systems*, 20(4), 1562–1573. doi: 10.1109/TITS.2018.2853264.

Hellström, E., Ivarsson, M., Åslund, J., and Nielsen, L. (2009). Look-ahead control for heavy trucks to minimize trip time and fuel consumption. *Control Engineering Practice*, 17(2), 245–254.

Henriksson, M., Flärdh, O., and Mårtensson, J. (2017). Optimal Powertrain Control of a Heavy-Duty Vehicle Under Varying Speed Requirements. In *2017 IEEE 20th International Conference on Intelligent Transportation Systems (ITSC)*, 1922–1927. Yokohama.

Heywood, J.B. (1988). *Internal combustion engine fundamentals*. 1. McGraw-Hill.

Kirches, C., Sager, S., Bock, H.G., and Schlöder, J.P. (2011). Time-optimal control of automobile test drives with gear shifts Christian. *Optimal Control Applications and Methods*, 32(3), 298–312. doi:10.1002/oca. URL `http://doi.wiley.com/10.1002/oca.939`.

Li, S.E. and Peng, H. (2011). Strategies to Minimize Fuel Consumption of Passenger Cars during Car-Following Scenarios. In *2011 American Control Conference*, 2107–2112. San Francisco.

Löfberg, J. (2004). YALMIP : a toolbox for modeling and optimization in MATLAB. In *2004 IEEE International Symposium on Computer Aided Control Systems Design*, 284–289. Taipei. doi: 10.1109/CACSD.2004.1393890.

Qian, X., Altché, F., Bender, P., Stiller, C., and de La Fortelle, A. (2016). Optimal Trajectory Planning for Autonomous Driving Integrating Logical Constraints : A MIQP Perspective. In *2016 IEEE 19th International Conference on Intelligent Transportation Systems*, 205–210. Rio De Janeiro.

Scania CV AB (2012). Scania Active Prediction. Technical Report December. URL `https://www.scania.com/group/en/event/pressroom-scania-active-prediction/`.

Scania CV AB (2013). Scania utilises gravity to save fuel. Technical report. URL `https://www.scania.com/group/en/scania-utilises-gravity-to-save-fuel-3/`.

TNO (2015). Cost-benefit analysis of options for certification , validation , monitoring and reporting of heavy-duty vehicle fuel consumption and CO2 emissions. URL `https://ec.europa.eu/clima/sites/clima/files/transport/vehicles/ heavy/docs/tno_2014_interim_report_en.pdf`.

Wang, Y., Schutter, B.D., Ning, B., Groot, N., and Boom, T.J.J.V.D. (2011). Optimal Trajectory Planning for Trains Using Mixed Integer Linear Programming. In *2011 14h International IEEE Conference on Intelligent Transportation Systems*, 1598–1603. Washington DC. doi:10.1109/ITSC.2011.6082884.

Xu, S., Li, S.E., Zhang, X., Cheng, B., and Peng, H. (2015). Fuel-Optimal Cruising Strategy for Road Vehicles with Step-Gear Mechanical Transmission. *IEEE Transactions on Intelligent Transportation Systems*, 16(6), 3496–3507. doi:10.1109/TITS.2015.2459722.